GEODESY AND CARTOGRAPHY
Vol. 65, No 1, 2016, pp. 41-53

DOI: 10.1515/geocart-2016-0007

Neural networks for the generation of sea bed models using airborne lidar bathymetry data

Tomasz Kogut[1], Joachim Niemeyer[2], Aleksandra Bujakiewicz[1]

[1] Koszalin University of Technology
Department of Geoinformatics
2 Śniadeckich St., 75-453 Koszalin, Poland
e-mail: tomasz.kogut@tu.koszalin.pl; abujak7@wp.pl

[2] Leibniz Universität Hannover
Institute of Photogrammetry and GeoInformation
D-30167 Hannover, 1 Nienburger St., Germany
e-mail: niemeyer@ipi.uni-hannover.de

Received: 1 December 2015 / Accepted: 30 January 2016

Abstract: Various sectors of the economy such as transport and renewable energy have shown great interest in sea bed models. The required measurements are usually carried out by ship-based echo sounding, but this method is quite expensive. A relatively new alternative is data obtained by airborne lidar bathymetry. This study investigates the accuracy of these data, which was obtained in the context of the project 'Investigation on the use of airborne laser bathymetry in hydrographic surveying'. A comparison to multi-beam echo sounding data shows only small differences in the depths values of the data sets. The IHO requirements of the total horizontal and vertical uncertainty for laser data are met. The second goal of this paper is to compare three spatial interpolation methods, namely Inverse Distance Weighting (IDW), Delaunay Triangulation (TIN), and supervised Artificial Neural Networks (ANN), for the generation of sea bed models. The focus of our investigation is on the amount of required sampling points. This is analyzed by manually reducing the data sets. We found that the three techniques have a similar performance almost independently of the amount of sampling data in our test area. However, ANN are more stable when using a very small subset of points.

Keywords: Airborne Lidar Bathymetry, interpolation, neural networks, inverse distance weighting, Delaunay triangulation

1. Introduction

In recent years, we have seen increased request for 3D data, which evolved not only in the direction of improving the accuracy and collecting a greater amount of data, but also in shortening the time of their acquisition. Traditionally, sea bed models are based on data obtained from single- or multi-beam echo-sounder measurements. An

alternative to conventional data acquisition is airborne laser bathymetry (ALB), which is a promising technique of surveying the sea bed. ALB sensors use a green laser of 532 nm wavelength which can penetrate the water column. It is often combined with an infrared laser of 1064 nm wavelength, which is reflected at the water surface. The depth is determined by the two-way runtime between the reflections from the water surface and the solid ground underneath. Especially the pulse repetition rate and, thus, the point density have been significantly increased with the state-of-the-art sensors. Good results under optimal conditions were reported (Costa et al., 2009; Steinbacher et al., 2012). However, there are many limiting factors like water turbidity, waves, and reflectance conditions of the sea bed.

In order to guarantee the quality of the hydrographic data and hence to ensure the safe navigation of ships, the International Hydrographic Organization (IHO) published the Standards for Hydrographic Surveys S-44 (International Hydrographic Organization, 2008). The quality demands are categorized into four classes. Three of them describe the shallow water requirements in depth less than 100 m. The penetration depth of ALB is limited to only a few metres in the Baltic Sea due to turbidity. Correspondingly, these data must at least meet the constraints defined in Order 1b to be used for an operational application in hydrographic surveying. To fulfil this category at least one Lidar spot located in a 5×5 m grid cell is required, whereas the detection of obstacles is not necessary.

An increase of human activities in shelf and coastal water areas such as gas pipeline or offshore wind turbines comes along with the requirement of a better understanding of the sea bed variability. For this reason, the interest on accurate sea bed models increases. Nowadays, depth measurements are usually performed by acoustic systems mounted on the ship (Brouwer, 2008). However, in particular the very shallow water regions are not accessible for ships resulting in data gaps in the transition zone between land and water. Common interpolations methods have problems with the interpolation of sparsely distributed data points. Therefore, improved methods are required. In case of topographic terrain modelling, Gumus et al. (2013) demonstrated that artificial neural networks are particularly suitable to handle data sets with variable point distributions. An artificial neural network is a powerful framework which has been shown to provide good results in many applications such as pattern recognition, clustering, function approximation, and optimization tasks (Jain et al., 1996). Due to these advantages we introduce neural networks for the generation of sea bed models in this paper. Bathymetric data is often irregularly distributed or shows some small data gaps. For this reason, an experiment was conducted in which the amount of sampling points in the point clouds was randomly reduced.

2. Methodology

The main goal of this paper is to compare three interpolation methods with respect to their applicability of generating digital sea bed models from varying ALB point

cloud densities. This investigation comprises the supervised artificial neural networks, on one hand, and the two conventional approaches of inverse distance weighting as well as Delaunay triangulation, on the other hand. They are described shortly in the following subsections.

2.1. Artificial neural network (ANN)

In general, an artificial neural network is a computing system made up of a number of simple, highly interconnected units, which process information by their dynamic state response to external inputs (Caudill, 1989). The original inspiration for such a structure was the central nervous systems of animals, in particular the brain. Each artificial neural network works as system of interconnected neurons which send messages to each other. The connections between neurons have weights that are determined in an iterative training phase. Based on Fig. 1 the functionality of the technique as well as the important terms of artificial neural networks are explained:

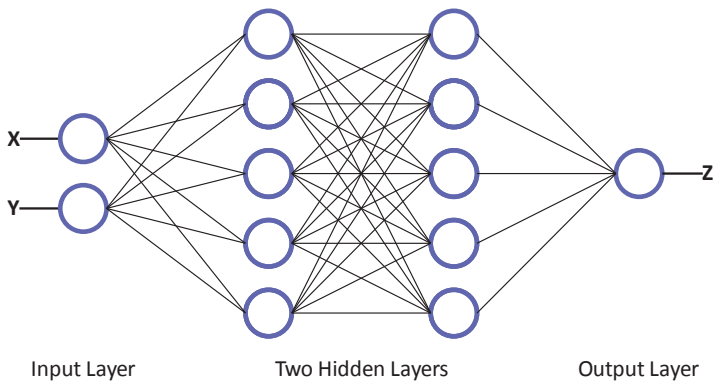

Fig. 1. Layout of the proposed artificial neural network

A multilayer feed-forward back propagation (MLBP) network is popular and often used for classification and pattern recognition tasks (Jain et al., 1996; Duda et al., 2000). The network consists of multiple (adaptive) layers of units, and it is not allowed to have cycles from later layers back to earlier layers (Bishop, 2007). The neurons are arranged in layers and a neuron of one layer is fully connected only with every neuron of the next layer, but not to any of the same layer, i.e., there are no intra-layer connections. The input layer distributes the input to the hidden layers and communicates with the external environment (Karsoliya, 2012). This layer represents the condition for which we train the neural network and every input neuron represents one independent variable. The output of the first layer is propagated through the hidden layer(s) of the net (Stefko, 2008), which are neither input nor output units, and their activations are not directly "seen" by the external environment (Duda et al.,

2000). The activation function is the process that happens after the input is presented to the neuron. The results determine the value of the next neuron in the following layer in the network (Bell, 2014). The hidden layer is the collection of neurons which have the activation function applied and the value of each neuron is multiplied by the weight. The resulting weight values are added and the weighted sum is transferred to the output layer, which accepts weights and adjusts them.

As shown in Fig. 1, our neural network has two hidden layers with two input units represented by the x- and y-coordinates of the ALB data. A subset of the point cloud is used for training data to generate a grid model of the sea bed. It is trained with the Levenberg-Marquardt algorithm (Levenberg, 1944; Marquardt, 1963; Hagan et al., 1994; Duda, 2000) and the adaptive learning rate is gradient descent with momentum weight and a bias learning function (Bai et al., 2009). The mean-square error is used as a criterion of the network training. The calculations are made with the software MatLab.

2.2. Inverse Distance Weighting (IDW)

IDW is a type of interpolation method calculating the height information of unknown points with a weighted average of the values available at the known points (Azpurua et al., 2010). The basic assumption is that close points have a greater influence on the interpolation than more distant points. Hence, the weights are a function of distances from a single ALB point to the interpolation points. The z-value can be calculated by the following equation

$$z = \frac{\sum_{i=1}^{n} \frac{z_i}{d_i^p}}{\sum_{i=1}^{n} \frac{1}{d_i^p}} \quad , \tag{1}$$

where d_i is a distance between the unknown and known data points, and z_i is the observed elevation value of point i. The parameter p is a control rate that models, to check how rapidly the weights decrease with increasing distance. It is typically set to $p = 2$ (Bagheri et al., 2014). Calculations concerning this part were made in SagaGis 2.1.4 (64-bit).

2.3. Delaunay Triangulation

Delaunay triangulation is another popular interpolation method, which represents the data by a triangulated irregular network (TIN). Thus, the results obtained by this method are denoted by 'TIN' in this paper. It creates a surface formed by triangles connecting the nearest neighbour points in order to determine the unknown height

value. It has been shown that TIN models are a good way to regularly sample data for terrain reconstruction (Zhong et al., 2008). The algorithm of Delaunay Triangulation was described by de Berg et al. (2008). The z-value of point *i* in the triangle *abc* can be calculated by the following equation (Hu et al., 2009)

$$z_i = \omega_a Z_a + \omega_b Z_b + \omega_c Z_c, \quad (2)$$

where $\omega_a + \omega_b + \omega_c = 1$, $\omega_a, \omega_b, \omega_c > 0$. The weights $\omega_a,\omega_b,\omega_c$ are the areal proportions of the sub-triangles constructed using *i*. Let *s* be the total area of the triangle *abc*, and s_a,s_b,s_c be the areas of the sub-triangles, then the proportions result to $\omega_a = s_a/s$, $\omega_b = s_b/s$, $\omega_c = s_c/s$. In our project the Delaunay Triangulation was executed in SagaGis 2.1.4 (64-bit).

3. Experiments

The aims of our investigations are: (1) to analyze the vertical accuracy of ALB data, (2) to generate sea bed elevation models from these data of varying point density using neural networks, and (3) to compare the quality of neural networks to common interpolations methods. A model created from multi-beam data serves as a ground truth for the accuracy assessment of the individual results. This section presents the experiments to evaluate the performance of our research. The study area is characterized in Section 3.1. Section 3.2 is dedicated to the evaluation of the vertical depth accuracy of the collected ALB data. Section 3.3 presents the comparison and the results of the three different interpolation methods.

3.1. Data

The data used for our research was obtained in the project 'Investigation on the use of airborne laser bathymetry in hydrographic surveying', carried out in the frame of a cooperation of the Federal Maritime and Hydrographic Agency (BSH) of Germany and the Institute of Photogrammetry and GeoInformation, Leibniz Universität Hannover (Germany). The test site for this study is located in the Baltic Sea, about 25 km North of Rostock (Germany), and comprises the artificial reef Rosenort (Fig. 2) at a depth of approx. 6 m. The area of the test region is 38,555 m^2 and 99,446 sea bed points were recorded. The airborne laser bathymetry data acquisition was conducted by TopScan GmbH in September 2013 with an AHAB Chiroptera sensor in an altitude of 400 m. The sensor works with a combination of a green laser (λ=532 nm) and an infrared laser (λ=1064 nm). As specified by the manufacturer, a typical measurement ranges to one and a half Secchi depth under good conditions, and the pulse repetition rate was set to 35 kHz (AHAB, 2013). The Secchi depth is the maximum depth at which the human eye can detect a test object (disk) in water and is related to its

turbidity. In addition to the ALB data also multi-beam data was gathered by the BSH Rostock in September 2013. They provided a DTM of 1 m resolution, which is used as a reference in our investigation.

In the test area four groups of obstacles are located on the sea bed, namely the parts of the artificial reef Rosenort consisting of various stony materials. Unfortunately, there are gaps in the ALB data exactly at the positions of the obstacles, and hence almost no 3D information about these objects could be inferred by ALB in this case. The four gaps with a length of 10-15 m and a width of 5-10 m each can be detected easily in the point cloud (Fig. 3A). This problem could be caused by the underwater vegetation growing on the top of the obstacles, leading to insufficient reflections of the laser signal. Another possible explanation could be that the echoes from the objects were incorrectly identified as noise and thus they were eliminated in the post-processing. These observations are already mentioned in Niemeyer et al. (2014). We will focus on this problem in our future work to identify the reasons.

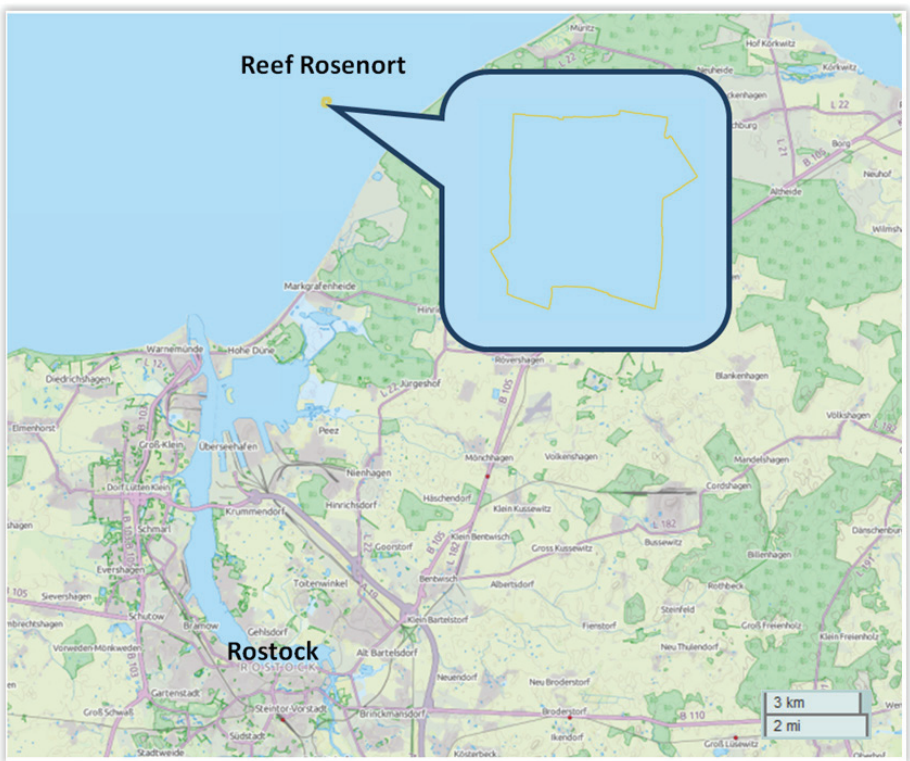

Fig. 2. Test area (OpenStreetMap)

3.2. Depth accuracy

The accuracies of each interpolation method are carried out by calculating the differences of the z-values between each grid model and the multi-beam data. The error can be determined by using the RMSE (root-mean-square error) rate, which is expressed as follows:

$$RMSE = \sqrt{\frac{\sum_{j=1}^{n}(z_j^{ALB} - z_j^{MB})^2}{n}} \tag{3}$$

where z^{ALB} are the interpolated z-values of the ALB data, z^{MB} are the height values from multi-beam grid, and n is the number of grid cells in the models (which is identical for the multi-beam and the interpolated ALB models).

As explained above, airborne laser bathymetry must meet the requirements of IHO S-44 Order 1b. The maximum allowable total horizontal uncertainty (THU) and the total vertical uncertainty (TVU) are defined by

$$THU_{max} = 5\ m + 5\%\ \text{depth}, \tag{4}$$

$$TVU_{max} = \sqrt{(0.5\ m)^2 + (0.013 * depth)^2}. \tag{5}$$

For each parameter a 95 % confidence level must be fulfilled.

The evaluation of the depth accuracy of the collected ALB data is an important task for further analysis presented in this paper. Therefore, only the points classified as *sea bed* are investigated. In our case the IHO requirements of the total horizontal and vertical uncertainty for laser data are 5.25-5.37 m (THU) and about 0.5 m (TVU), respectively, according to equations 4 and 5. However, in the present work the accuracy assessment was focused only on TVU, because there was not sufficient structure in the data to validate also the horizontal accuracy. The ALB data (Fig. 3A) are compared to the multi-beam echo sounding data (Fig. 3B) by computing the depth difference for each ALB sea bed point and its nearest echo sounding grid point.

The results of the differences between the laser point cloud and the reference DTM reveal that both techniques ALB and echo sounding lead to comparable results. They are depicted in Fig. 3. The majority (99.9 %) of the laser points satisfy the total vertical uncertainty threshold which is ±0.5 m. This shows that both data sets match well and hence the ALB points have a good vertical accuracy.

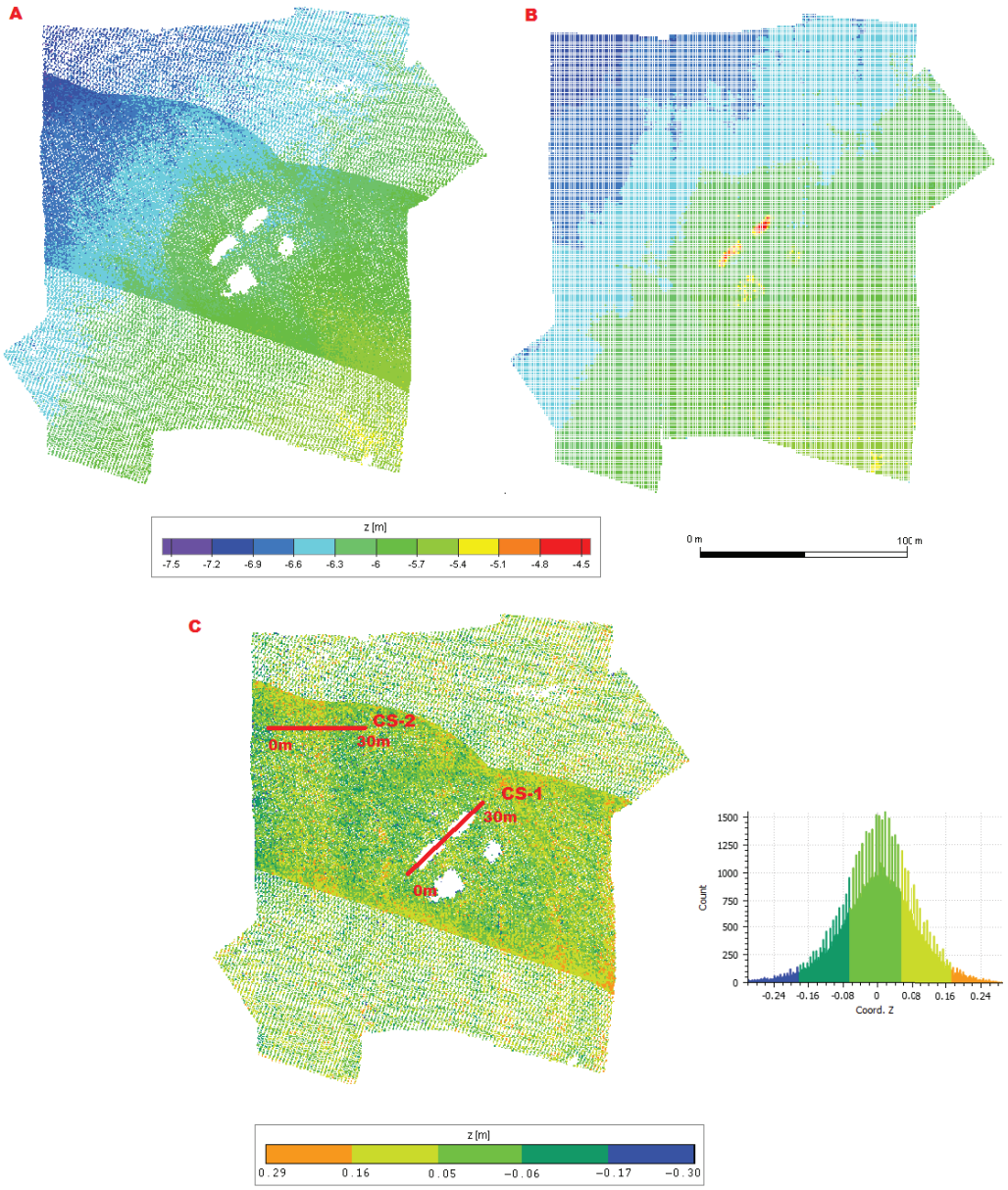

Fig. 3. A) Airborne laser bathymetry point cloud of the sea bed;
B) Grid model of the sea bed from multi-beam measurements;
C) difference between ALB data and multi-beam data with the corresponding histogram of the vertical differences. CS-1 and CS-2 show the positions of the 2D profiles used for Fig. 4 and 5.

3.3. Analysis of results

The first experiment showed a good vertical accuracy of the laser points, enabling the next step of our investigation: the comparison of three different methods for the generation of a sea bed DTM. In this section the accuracy of the different approaches with respect to varying point densities is analyzed. For that purpose, random subsets of 50%, 25%, 10%, 5%, and 1% of all points in the point cloud are drawn to form data sets with reduced point densities, which are summarized in Table 1:

Table 1. Point densities of input point clouds

Point cloud size	100 %	50 %	25 %	10 %	5 %	1 %
Point density (pts/m²)	2.58	1.29	0.64	0.26	0.13	0.03

These artificially reduced point clouds are then used to analyze the influence of the point densities on the investigated interpolation methods. They serve as training data for the neural network approach (to learn the weights) as well as input data for the unsupervised methods Inverse Distance Weighting and Delaunay triangulation. For each density level the same subsampled point cloud is used for all three interpolation methods to generate a new sea bed raster model of 1 m resolution in order to enable a convincing comparison. After that, each model is compared to the multi-beam elevation model with 1 m grid size, which was provided by the BSH.

The results of all interpolation methods show that they are almost similar for all models, independent of the point densities. For each data set the RMSE is approximately 0.1 m, the mean difference is about 0.01 m. In the case of the TIN interpolation a restriction has to be taken into account. Due to the distribution of the randomly selected points it may appear that not all pixels of the sea bed model are covered by a triangle of the TIN. Consequently, it is not possible to interpolate a depth value for these pixels and hence they have to be ignored in the evaluation of the comparison with the multi-beam model. The number of ignored pixels increases from 55 to 1922 with a decreasing amount of Lidar points because the covered area of the generated TIN triangles is likely to be reduced in this case.

In addition, for a better presentation of the properties of the resulted models, two elevation profiles are shown in Fig. 4 and 5. The first profile is generated from models based on all points and comprises the two obstacles (Fig. 3C, CS-1) on the sea bed. There are almost no ALB points located on the obstacles. Therefore, the interpolation is based only on points which are situated next to an obstacle leading to non-realistic results. However, in case of the method TIN, a small peak of approximately 20% of the object's height can be observed at the corresponding locations in Fig. 4. The reason is, that the heights of all samples are directly used to perform the triangulations

between the points. In this case some (few) points located on the edges of the obstacles were actually detected and thus taken into account for the interpolation with TIN. The other two methods ANN and IDW also perform a smoothing of the data. This effect leads to an elimination of the small remaining peaks of the obstacles. Note that the oceanic relief in the study area is quite flat and does not show much undulation of the ground despite of the obstacles. In future works, test sites with more variation in depth will be investigated.

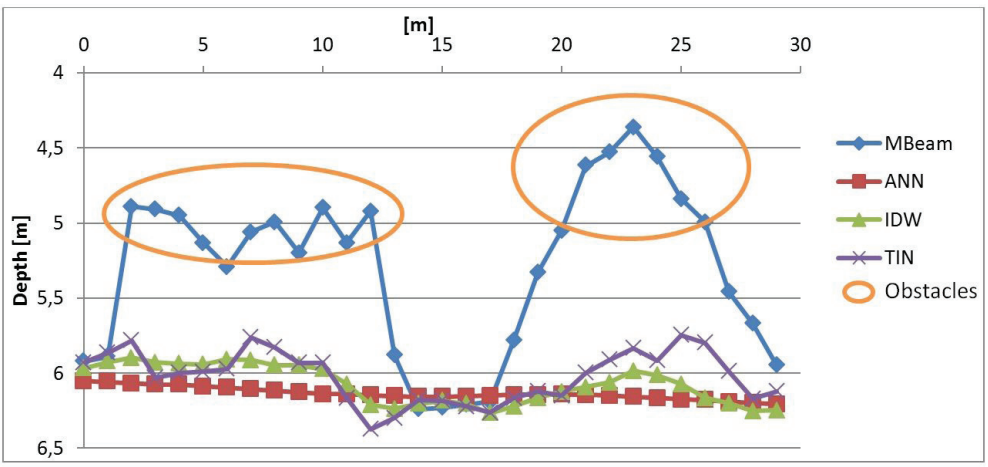

Fig. 4. Profile CS-1 of DTMs obtained by all methods showing the underwater obstacles based on the interpolation of 100% of the points. MBeam- multibeam data, ANN- Artificial neural network, IDW- Inverse Distance Weighting, TIN- Delaunay Triangulation

The second cross-section profile (Fig. 5) shows a randomly sampled location (Fig. 3C, CS-2) on the sea bed. The model was defined on only 1 % of the points. In this case, the traditional interpolation methods are unstable and generate many peaks in both directions of the z-axis. In contrast to that the model generated by the ANN is more stable with only smooth changes, and the surface is close to that of the multi-beam data. Although the ANN simplified edges, it is a sophisticated predictor of the curvature of the sea bed. An advantage of ANN compared to TIN and IDW is that the input data are unrelated to the interpolated data (the result only depends on the weights of the neurons) and therefore the ANN-model is smooth. This effect is positive when having data of varying quality.

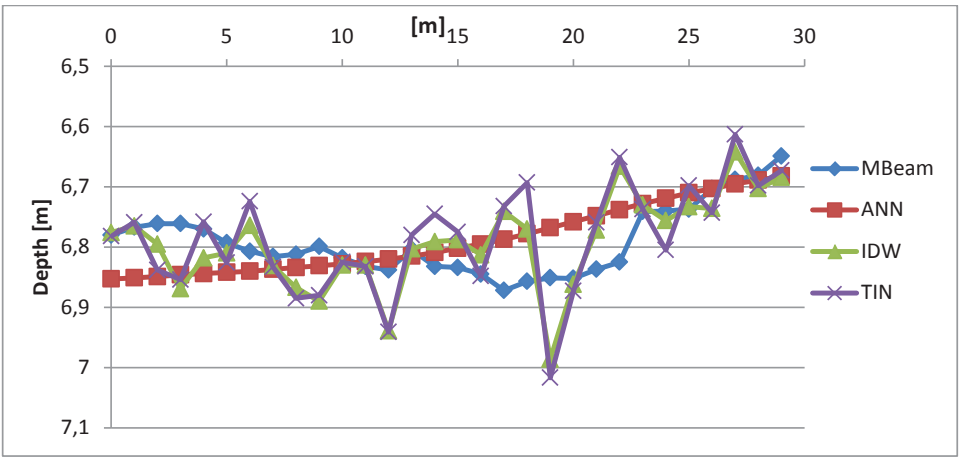

Fig. 5. Profile CS-2 of DTMs obtained by all methods showing a randomly sampled location based on the interpolation of only 1 % of the points

4. Conclusion and outlook

This paper investigates the vertical accuracy of the sea bed point cloud obtained by airborne laser bathymetry (ALB), on the one hand. It appears that the data acquired by the Sensor AHAB Chiroptera meet the international demands in terms of the vertical accuracy for the small test site with a water depth of about 6 m. On the other hand, three techniques for the interpolation of terrain models describing the sea bed are analyzed with respect to a reference model generated from multi-beam echo-sounding data. For this study a new application of the artificial neural networks (ANN) is presented. The resulting DTM is compared to those obtained by the two traditional interpolation methods Inverse Distance Weighting and Delaunay triangulation. Also an experiment with a varying amount of input data for the three methods is carried out. We found that ANN are more stable in the case of relatively few points. The elevations of this model are close to those of the multi-beam model, and hence it can be used as a basis for further applications. Furthermore, a comparison depicted that both, the amount of training data as well as the interpolation method, do not have a great impact on the accuracy of the interpolated model in our flat test study. We aim to carry out a similar comparison in areas with more changes of the sea bed topography to yield more expressive results.

The detection of underwater obstacles was challenging in the tests because the laser pulses were reflected only weakly when they illuminated objects leading to gaps in the data. In further work we want to concentrate on this issue and analyze the full waveforms to extract more points describing the underwater obstacles on the sea bed.

Acknowledgement

The data used in this study was obtained in the context of the project 'Investigation on the use of airborne laser bathymetry in hydrographic surveying', which was funded by the Federal Maritime and Hydrographic Agency (BSH) of Germany under project number 10019311. The support and the data are gratefully acknowledged.

References

Airborne Hydrography AB, (2013). *Chiroptera – Technical Specification.* http://www.airbornehydrography.com/chiroptera (29.4.2013).

Azpurua, M. and Ramos, K. (2010). A comparison of spatial interpolation methods for estimation of average electromagnetic field magnitude. *Progress In Electromagnetics Research M*, Vol. 14: 135-145.

Bagheri, H., Sadeghian, S. and Sadjadi, S. Y. (2014). The Assessment of using an Intelligent Algorithm for the Interpolation of Elevation in the DTM Generation. *PFG – Photogrammetrie, Fernerkundung, Geoinformation*, Vol. 3 (2014): 197–208.

Bai, Y., Zhang, H. and Hao, Y. (2009). The performance of the backpropagation algorithm with varying slope of the activation function. *Chaos, Solitons & Fractals*, Vol. 40(1): 69–77.

Bell, J. (2014). *Machine Learning: Hands-On for Developers and Technical Professionals*, Wiley, 95.

Bishop, C. (2007). Pattern Recognition and Machine Learning. Springer.

Brouwer, P.A.I. (2008). *Seafloor classification using a single beam echosounder*, TU Delft.

Caudill, M. (1987). Neural networks primer, part I, *AI Expert*, Vol. 2(12) pp. 46 – 52.

Costa, B. M., Battista, T. A. and Pittman, S. J. (2009). Comparative evaluation of airborne LiDAR and ship-based multibeam SoNAR bathymetry and intensity for mapping coral reefecosystems, *Remote Sensing of Environment*, 113(5): 1082-1100.

de Berg, M., Cheong, O., van Kreveld, M. and Overmars, M. (2008). *Computational Geometry: Algorithms and Applications,* Springer, 191-218.

Duda, R O, Hart, P. and Stork, D. (2000). *Pattern Classification. Second Edition,* Wiley-Interscience.

Gumus, K. and Sen, A. (2013). Comparison of spatial interpolation methods and multi-layer neural networks different point distributions on a digital elevation model, *Geodetski Vestnik,* Vol. 57(3): 523.

Hagan, M.T. and Menhaj, M.B. (1994). Training feedforward networks with the Marquardt algorithm, *IEEE Transactions on Neural Network*, Vol. 5, pp. 989–993.

Hu, P., Liu, X. and Hu, H. (2009). Accuracy Assessment of Digital Elevation Models based on Approximation Theory, *Photogrammetric Engineering and Remote Sensing*, Vol. 75, No.1: 49-56.

International Hydrographic Organization, (2008). *IHO Standards for Hydrographic Surveys,* Special Publication N 44, 5th Edition.

Jain, A.K., Mao, J. and Mohiuddin, K. (1996). Artificial Neural Networks: A Tutorial. Computer, Vol. 3, *IEEE*, 31-44.

Karsoliya, S. (2012). Approximating Number of Hidden layer neurons in Multiple Hidden Layer BPNN Architecture, *International Journal of Engineering Trends and Technology.*

Levenberg, K. (1944). A method for the solution of certain non-linear problems in least squares, *Quarterly Journal of Applied Mathematics*, Vol. II(2): 164–168.

Marquardt, D. W. (1963). An algorithm for least-squares estimation of non-linear parameters, *Journal of the Society for Industrial and Applied Mathematics*, Vol. 11(2): 431–441.

Niemeyer, J., Kogut, T. and Heipke, C. (2014). Airborne Laser Bathymetry for Monitoring the German Baltic Sea Coast, *Tagungsband der DGPF-Jahrestagung (Proceedings of the annual conference of the German Society for Photogrammetry, Remote Sensing and Geoinformation*), Vol. 23.

Stefko, K. (2008). Application of MLBP Neural Network for Exercise ECG Test Records Analysis in Coronary Artery Diagnosis, *Information Technologies in Biomedicine, Advances in Soft Computing,* Vol. 47, Springer, pp 179-183.

Steinbacher, F., Pfennigbauer M., Aufleger, M. and Ullrich, A. (2012). High resolution airborne shallow water mapping, *International Archives of the Photogrammetry, Remote Sensing and Spatial Information Sciences, Proceedings of the XXII ISPRS Congress*, Vol. XXXIX-B1, Melbourne, Australia, pp. 55–60.

Zhong, D., Liu J., Li M. and Hao, C. (2008). NURBS reconstruction of digital terrain for hydropower engineering based on TIN model, *Progress in Natural Science*, Vol. 18, Issue 11: 1409–1415.